IOP Conf. Series: Materials Science and Engineering **186** (2017) 012007 doi:10.1088/1757-899X/186/1/012007

Structural and optical properties of hydrothermally synthesized vanadium oxides nanobelts

I Derkaoui[1,3*], M Khenfouch[2,3], I Elmokri[1], B. M Mothudi [2], M. S Dhlamini[2], S. J Moloi[2], I Zorkani[1], A Jorio[1], M Maaza[4,5]

[1]University Sidi Mohammed Ben Abdellah, Faculty of Sciences Dhar el Mahraz, Laboratory of Solid state Physics, Group of Nanomaterials and Renewable Energies, PO Box 1796 Atlas Fez 30 000, Morocco
[2]UNISA university of South Africa, Department of Physics, College of Science, Engineering and Technology, Science Campus, Cnr Christiaan de Wet & Pioneer Avenue Florida 1709, Johannesburg, South Africa
[3]Africa Graphene Center, 2 Boekenhout street, Florida, Johannesburg, 1709 South Africa.
[4]Nanosciences African Network (NANOAFNET), iThemba LABS-National Research Foundation, 1 Old Faure road, Somerset West 7129, PO Box 722, Somerset West, Western Cape-South Africa
[5]UNESCO-UNISA Africa Chair in Nanosciences Nanotechnology, College of Graduate Studies, University of South Africa, Muckleneuk ridge, PO Box 392, Pretoria-South Africa

E-mail: derkaouiissam@gmail.com

Abstract. Nanostructured metal oxides have attracted a lot of attention recently owning to their unique structural advantages, and demonstrated promising chemical and physical properties for various applications. In this study, we report the structural and optical properties of vanadium oxide nanoparticles (VO-NPs) prepared via a hydrothermal method. Our results are revealing that the components of VO-NPs films are having a belt-like shape with a uniform size distribution. The nanobelts with very smooth and flat surfaces have a typical length of up to 1μm and a width of about 9-14 nm. Moreover, The UV-Visible spectroscopy revealed an excellent optical propertiesshowing clearly the good stoichiometry and crystallinity of our VO-NPs films. This synthesis method provides a new simple route to fabricate one-dimensional nanostructured metal oxides which is suitable for a large field of applications.

1. Introduction

Among the transition metal oxides, vanadium oxides have attracted special interest because of their coordination polyhedral and a wide range of oxidation states (from +2 to +5) in the vanadium-oxygen system [1]. Nanostructured vanadium oxides materials, such as nanorods, nanowires, nanotubes and nanobelts, have attracted considerable attentions because to both their distinctive geometries, specific physical and chemical properties that are different from the bulk materials due to their limited size and high density of corner or edge surface sites [2].

In the light of previous reports, vanadium oxides nanoparticles possessing unique electrical and optical properties, it was found to show high electronic conductivity arising from a mixed-valence V

$3^{+}/5^{+}$ and structural stability arising from increased edge sharing and the consequent resistance to lattice shearing during cycling [3]. Moreover, it can undergo a first-order transition from a high-temperature metallic phase to a low temperature semiconductor phase at around 68 °C that is the result of an atomic structural rearrangement, this temperature is increasing with decreasing the size of particles [4]. Owing to their important properties they exhibit potential application in fabricating nanoscale electronic, optical, electrochemical, optoelectronic, and electromechanical devices [5,6]. Because of these attractive properties and applications, many different synthesis techniques have been developed for the synthesis of vanadium oxide nanoparticles. For instance, sol–gel [7], chemical vapor deposition [8] and pulsed laser ablation [9]. Hydrothermal synthesis is found to be a suitable method to obtain vanadium oxide nanoparticles. This technique is ideal for the processing of very fine powders and films having excellent reproducibility, high purity, narrow particle size distribution and controlled morphology [10].

In this work, we are presenting the structural and optical properties of nanostructured metal oxide nanoparticles which include growth mechanism description and interactions discussion. In this sense, transmission electron microscopy (TEM), X-ray diffraction (XRD), Fourier transform infrared spectroscopy (ATR-FTIR)and ultraviolet-visible spectrum (absorbance/reflectance) were investigated.

2. Samples preparation

2.1 Synthesis of VO-NPs

All of the chemical reagents were analytical grade. They were purchased from Acros Organics and used without further purification. The detailed for the synthesis was as follows.

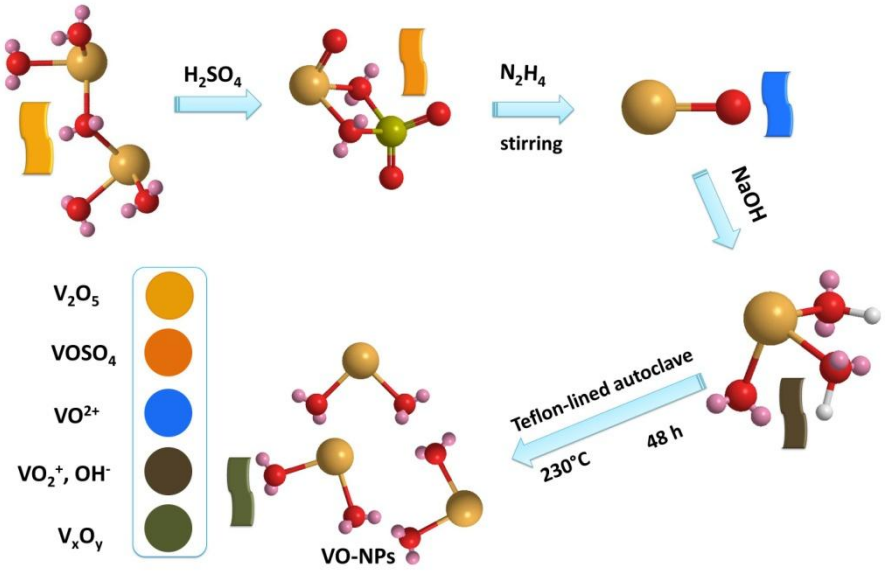

Figure 1. Growth mechanism of vanadium oxides nanoparticles.

VO-NPs were synthesized using a hydrothermal procedure. In a typical synthesis addition of 0.75 ml of sulphuric acid, H_2SO_4, into an aqueous suspension of 0.45g of V_2O_5 was followed by the addition of hydrazine hydrate(N_2H_4-$2H_2O$). After stirring thoroughly, the solution's color changed from yellow (V^{5+} valence state) to blue, indicating the reduction of V^{5+} to yield V^{4+} ions in solution. The pH of the resultant strongly acidic blue VO^{2+} solution was then adjusted to pH≈5 by adding NaOH solution. Heat could also be applied to the solution while adding NaOHsolution. A gray to

brown precipitate was formed during the addition of NaOH solution. Afterward, the suspension was transferred into a 25 mL Teflon-lined stainless autoclave. The autoclave was maintained at 230°C for 48 h and then air cooled to room temperature. The resulting dark blue precipitates were collected and washed with distilled water and ethanol several times and then dried at 60°C under vacuum for few hours(Figure 1).

2.1 Characterization

In this study, transmission electron microscopy (TEM) is employed to observe the morphology of VO-NPs, XRD pattern was obtained from a Rigaku Smart Lab system using Cu Kα (λ=1.54178 Å), ATR-FTIR spectrum was obtained using a Broker Vertex 70 with ATR system, Raman spectrum was obtained using a Bruker Multi Ram with and excitation wavelength of 1064 nm. Finally, Uv-Vis (absorbance/ reflectance) spectrum was carried out using Perkin Elmer lambda 1050 UV/Vis/NIR spectrometer.

3. Results and discussion

3.1TEM measurements

To investigate the morphology of vanadium oxides nanoparticles, TEM images have been taken and shown in Figure 2a. Figure 2a shows a typical panoramic TEM image of the VO-NPs film, where the components are nanobelts with a uniform size distribution. The nanobelts with very smooth and flat surfaces have a typical length of up to 1μm and a width of about 9-14 nm.

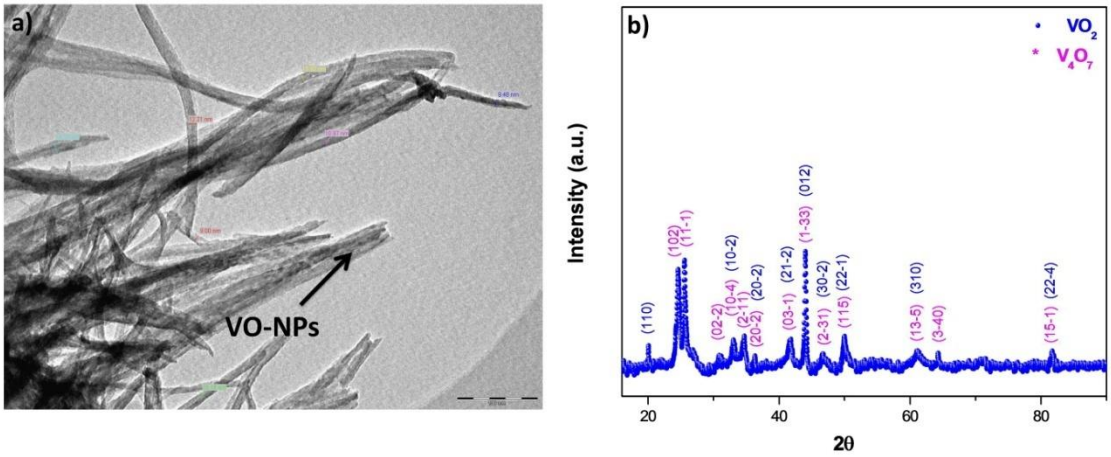

Figure 2. (a) TEM images of VO-NPs nanobelts, (b) X-rays diffraction pattern of VO-NPs.

3.2X-ray diffraction

Figure 2 b shows the XRD pattern of the as-prepared vanadium oxide nanoparticles. This pattern revealed the existence of the two phases tetravanadium septoxide (V_4O_7) and vanadium dioxide (VO_2). Strong diffraction peaks were observed at Bragg angles 24.61°, 25.53°, 30.98°, 33.03°, 34.63°, 36.35°, 41.65°, 43.97°, 46.59°, 49.79°, 61.29° and 81.79°, which they could be assigned to the (102) (11$\bar{1}$) (02$\bar{2}$) (10$\bar{4}$) (2$\bar{1}$1) (20$\bar{2}$) (03$\bar{1}$) (1$\bar{3}$3) (2$\bar{3}$1) (115) (13$\bar{5}$) and (15$\bar{1}$) planes, which can be readily indexed to the Triclinic crystalline phase (Space group 2 : A^{-1}) of V_4O_7 with the lattice constants a=5.456640 A°, b=6.941393 A° and c= 12.139513 A° (**α** =95.099998 **β**=122.599998

γ =109.250000) (ICDD card N° 1008024).Furthermore, the diffraction peaks at Bragg angles 20.16°, 33.03°, 36.35°, 41.65°, 43.97°, 46.59°, 49.79°, 61.29° and 81.79° are assigned to the (110) (10$\bar{2}$) (20$\bar{2}$) (21$\bar{2}$) (012) (30$\bar{2}$) (22$\bar{1}$) (310) and (22$\bar{4}$) planes, this series can be perfectly indexed to the Monoclinic(b) crystalline phase (Space group 14 : P121/c[1]) of VO_2 with lattice constants a=5.849727 A°, b=4.600944 A°, c= 5.474888 A° and β=122.599998(ICDD card N° 9009089), revealing that the V^{5+} ions in V_2O_5 have been reduced to V^{4+} ions by the hydrazine in the reaction. No peaks of any other phases or impurities were detected in the spectra, which mean that the products are mainly composed of vanadium oxides nanoparticles. In addition, the plot in Figure 3 present an estimation of these V_4O_7 andVO_2 nanoparticles size calculated using Hall method where the obtained size average was found to be 96 (56) and 94 (93) respectively.

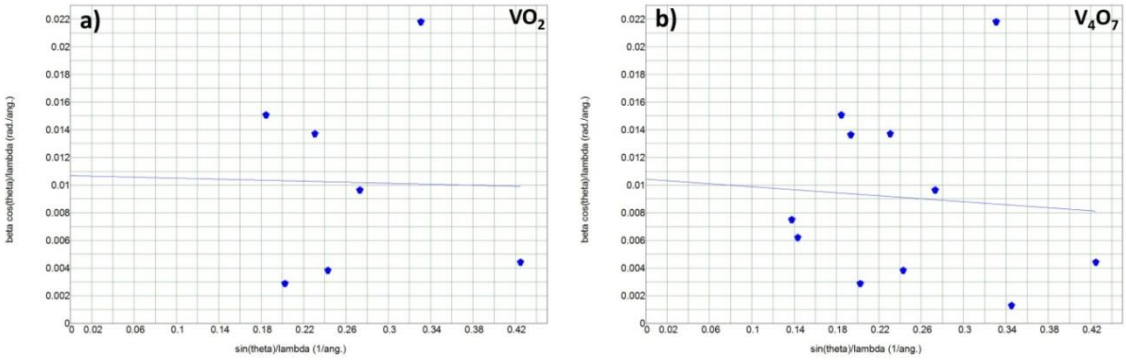

Figure 3. Size estimation in vanadium oxide nanostructures (a) and (b) of VO-NPs.

3.3 Fourier transform infrared spectroscopy

ATR-FTIR spectroscopy is one of the powerful tools for detecting the species on the nanostructures surface. As we can see VO-NPs (Figure 4) infrared spectrum has multiple bands, the two ones at 617 and 670 cm^{-1} are associated to the characteristic V-O-V octahedral bending modes [11]. Moreover, the peak located at 893 cm^{-1} is attributed to the coupled vibration V=O and V-O-V [12]. The characteristic peak at 910 cm^{-1} corresponds to V^{4+} terminal oxygen bonds (V^{4+} =O) and the peak at 1005 cm^{-1} which corresponds to V^{5+} terminal oxygen bonds (V^{5+} =O) becomes stronger [11,13]. The stretching vibrations of the V=O (vanadyl) bond is observed at 990 cm^{-1} while the band located at 1070 cm^{-1} is assigned to the oxidation state from V^{5+} to V^{4+}[12]. Therefore, the IR results are consistent with the formation of VO-NPs nanobelts which is in good agreement with the TEM observations.

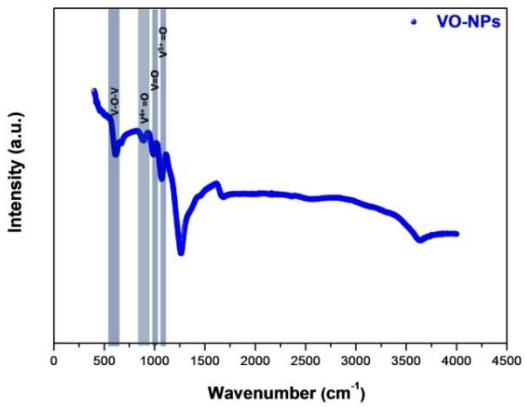

Figure 4. The ATR-FTIR spectrum of vanadium oxides nanoparticles.

3.4 UV-Vis spectroscopy

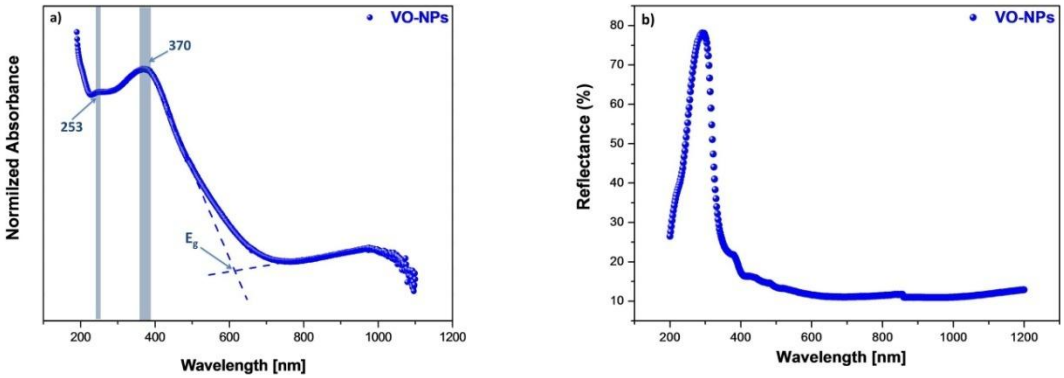

Figure 5. Uv-Vis optical spectra of the (a) VO-NPs absorbance and (b) VO-NPs reflectance.

Figure 5 shows the ultraviolet-visible spectra of VO-NPs films on glass substrates measured in the wavelength range 200-1000 nm. The absorbance spectrum of VO-NPs (Figure 5a) has two bands located at around 253 nm and 370 nm, the first should be assigned to charge transfer transition, involving oxygen and vanadium (IV) in tetrahedral coordination, present in isolated species [14,15]. The second broad band at 370 nm is attributed to octahedral V^{4+} species [14].The gap energy from Uv-visible spectrum absorbance can be determined at the tangent to the absorption front, and the width of the band gap is strongly dependent on the conjugation length. The optical band gap of VO-NPs nanobelts was found to be 3.33 eV which is higher than the band gap of vanadium oxide nanosheets reported by Wang (2.1 eV) [16]; This increment in the optical band may be attributed to the dimensional confinement effects of the VO-NPs [17,18].Figure 5b shows the reflectance spectrum of VO-NPs films. Reflectivity change was observed distinctly in the wavelength region 200-400 nm and slightly above 400 nm. In the wavelength region 200-400 nm, the VO-NPs films has a high reflectance (78%) showing clearly the good stoichiometry and crystallinity of the nanobelts which have an influence to enhanced the optical properties of vanadium oxides nanoparticles films.

4. Conclusion

To summarize, nanostructured vanadium oxides were successfully synthesized on glass substrates via a simple hydrothermal synthesis method. The structural investigations revealed the existence of two phases of VO-NPs while the vibrational properties are confirming the formation of these nanoparticles which assisted to the understanding of the growth mechanism. Moreover, our results showed that the geometrical shape of these vanadium oxides nanostructures is a belt with a uniform size distribution. The length and diameter of these nanobelts with very smooth and flat surfaces are 1μm and about 9-14 nm, respectively. Furthermore, the growth mechanism was found to have a great impact on the optical properties and strong absorption of Uv-Vis light of our VO-NPs nanobelts films. This study is focused on its offering of information which may assist to control the preparation of this nanostructured vanadium oxides and modulating their properties to enhance their efficiency then improve the performance of their applications including storage devices.

Acknowledgements

Special thanks to the Innovation city of USMBA (Morocco), Abdus Salam International Centre for Theoretical Physics (Trieste-Italy), Nanosciences African Network, University of South Africa Department of Physics, iThemba Labs (South Africa), African Laser Center and Africa Graphene Center.

References

[1] Livage J 2010*Materials*, **3** 4175-4195
[2] Fernandez-Garcia M, Martinez-Arias A, Hanson J C and Rodriguez J A 2004 *Chemical Reviews* **104** 4063-4104
[3] Lampe-Önnerud C, Thomas J O, Hardgrave M and Yde-Andersen S 1995 *Journal of Electrochemical Society* **142** 3648-3651
[4] Soltane L, SediriF and Gharbi N 2012 *Materials Research Bulletin* **47** 1615-1620
[5] Ji S D, Zhao Y G, Zhang F and P. Jin 2010 *Journal of* Crystal Growth **312** 282-286
[6] Ganganagappa N and Siddaramanna A 2012 *Materials Characterization* **68** 58-62
[7] Yin D C, Xu N K, Zhang J Y and Zheng X L 1996 *Journal of Physics. D: Applied Physics* **29** 1051-1057
[8] Manning T D, Parkin I P, Pemble M E, Sheel D and Vernardou D 2004 *Chemistry of Materials* **16** 744-749
[9] Kim D H and Kwok H S 1994 *Applied Physics Letters* **65** 3188-3190
[10] Byrappa K and Adschiri T 2007 *Progress in Crystal Growth and Characterization of Materials* **53** 117-166
[11] Sediri F and Gharbi N 2007 *Materials* Science *and* Engineering B **139** 114-117
[12] Pavasupree S, Suzuki Y, Kitiyanan A, Pivsa-Art S and S. Yoshikawa 2005 *Journal of Solid State Chemistry* **178** 2152-2158
[13] Lavayen V, O'Dwyer C, Cardenas G, Gonzàlez G and Sotomayor Torres C M 2007 *Mater. Res. Bull* **42** 674-685
[14] Murgia V, Torres E M F, Gottifredi J C and Sham E L 2006 *Applied Catalysis A* **312** 134–143
[15] Liu J and Xue D 2010 *Nanoscale Research Letters* **5** 1619-1626
[16] Wang Y T and Chen C H 2013 *Inorganic Chemistry* **52** 2550-2555
[17] Wang Y, Zhang Z, Zhu Y, Li Z, Vajtai R, Ci L and Ajayan P M 2008 *ACS Nano* **2** 1492-1496
[18] Liu J and Xue D 2008 *Advanced. Materials* **20** 2622-2627